Cancer Chemother Pharmacol (2016) 78:971–982
DOI 10.1007/s00280-016-3149-9

ORIGINAL ARTICLE

JD enhances the anti-tumour effects of low-dose paclitaxel on gastric cancer MKN45 cells both in vitro and in vivo

Cong Wang[1] · Ran Wang[1] · Kairui Zhou[1] · Saiqi Wang[1] · Junwei Wang[1] · Hongge Shi[1] · Yinhui Dou[1] · Dongxiao Yang[1] · Liming Chang[1] · Xiaoli Shi[1] · Ying Liu[1] · Xiaowei Xu[1] · Xiujuan Zhang[1] · Yu Ke[1] · Hongmin Liu[1]

Received: 12 June 2016 / Accepted: 26 August 2016 / Published online: 12 September 2016

Abstract
Background Gastric cancer is the third most common cause of cancer mortality worldwide, and paclitaxel (PTX) is one of the most widely used traditional drugs in gastric cancer therapy. However, the response to traditional therapy is limited by acquired chemo-resistance and side effects. Here, we establish a newly designed combination therapy consisting of a compound that is a structural variant of oridonin, i.e. Jesridonin (JD), and low-dose PTX for gastric cancer cells (MKN45) to investigate whether the anti-tumour activity of low-dose PTX could be enhanced when combined with JD.
Methods The interaction of JD and low-dose PTX was detected in MKN45 cells using the median-effect analysis method. The synergistic effect on cell viability and apoptosis was measured by MTT assay, colony formation assay, transient transfection, flow cytometry and Western blotting. The synergistic in vivo effect of JD plus low-dose PTX was evaluated in nude mouse xenograft models using H&E and TUNEL staining and Western blotting.
Results JD plus low-dose PTX showed a synergistic effect, as the combination indexes were less than 1. Additionally, a synergistic anti-proliferative and pro-apoptotic effect was detected for the combination of JD and low-dose PTX. The apoptotic mechanism induced by JD plus PTX revealed that the combination therapy synergistically activated the mitochondrial pathway.
Conclusion Our findings suggest that JD enhances the anti-tumour effect of low-dose PTX on gastric carcinoma cancer cells in both vitro and in vivo, accompanied by activation of the mitochondrial pathway, which may present a more effective therapeutic strategy in gastric cancer treatment.

Keywords JD · Paclitaxel · Combination therapy · Gastric cancer · Anti-tumour effect

Introduction

Gastric cancer is the world's fourth most common cancer and the third leading cause of cancer deaths worldwide [1, 2]. With approximately 1,000,000 new cases each year, gastric cancer is increasingly frequently diagnosed throughout the world. Additionally, more than 700,000 patients die of this disease because of the lack of validated screening programs and good treatment strategies [3]. Currently, modern combination therapies are preferred because of their benefit-to-risk ratio. This method has been adopted worldwide, although a gold standard has not yet been defined [4–8]. Combining drugs or reducing the dosage is a good method for resolving clinical problems, such as drug resistance and side effects. Paclitaxel (PTX) has clearly demonstrated activity against gastric cancer, mainly through its induction of mitotic catastrophe [9–11]. Although the anti-tumour effects of PTX are commonly exhibited through its interference with mitosis, there is compelling evidence suggesting that PTX acts through different apoptotic mechanisms, such as the PI3K/AKT pathway, the mitochondrial pathway and the EGFR

Cong Wang and Ran Wang have contributed equally to the research.

✉ Hongmin Liu
liuhm@zzu.edu.cn

[1] Key Laboratory of Advanced Pharmaceutical Technology, Ministry of Education of China, Co-innovation Center of Henan Province for New Drug R & D and Preclinical Safety, Zhengzhou University School of Pharmaceutical Sciences, 100 Kexue Avenue, Zhengzhou 450001, Henan, People's Republic of China

pathway [12–17]. Jesridonin (JD) is a derivative of oridonin, which is an active diterpenoid compound found in *Rabdosia rubescens* and has been widely used in the treatment of various cancers [18, 19]. There is a substantial amount of evidence indicating that oridonin may effectively improve survival and cancer response while having a low toxicity [20]. Nevertheless, the function of oridonin is limited by its poor chemical stability and cell membrane permeability. Thus, to obtain a compound with good chemical stability and cell membrane permeability, JD was designed by modifying and optimising the structure of oridonin. We have previously reported that JD has good anti-tumour activity and low toxicity in human oesophageal carcinoma cells [19].

In this study, we aimed to investigate the effect of a new combination strategy with PTX on gastric cancer cells. Collectively, our results suggest that the combination of JD and low-dose paclitaxel is a promising candidate therapeutic strategy in gastric cancer because the interaction between low-toxicity JD and low-dose PTX exhibits a synergistic anti-tumour effect not only in vitro but also in vivo. Additionally, the molecular mechanism underlying the anti-tumour activity was investigated in detail.

Results

JD and PTX monotherapy decreases the viability of MKN45 cells in a time- and concentration-dependent manner

The cell viability was detected by MTT assay. MKN45 cells were exposed to JD for 24, 48 and 72 h at increasing concentrations ranging from 2.5 to 150 μM, and negative control cells were incubated without JD. For PTX, the incubation time was the same as with JD, but the concentrations ranged from 0.15 to 25 μM. The corresponding viability was plotted against each concentration, represented by at least three independent experiments. The correlation between dosage and viability was illustrated and indicated that both JD and PTX decreased the viability of MKN45 cells in a time- and concentration-dependent manner (Fig. 1b, c). The IC_{50} values for JD and PTX were also calculated (Table 1).

Combination treatment with JD and low-dose PTX synergistically decreases the viability of MKN45 cells

We further assessed whether JD could enhance the efficacy of PTX. For this assessment, MKN45 cells underwent a combination treatment for 24 h with PTX (5 nM) plus JD at various concentrations (JD: 10, 15, 20, 25, 30 and 40 μM), and the viabilities were examined by MTT assay. The effect of each drug combination treatment was compared with the effect of treatment with either agent alone and of the control without any drug treatment (Fig. 1d). Briefly, compared to single-agent treatment, the cell viability resulting from combination therapy was reduced to varying degrees. Next, the combination index (CI) values of JD plus PTX were evaluated by the median-effect method proposed by Chou and Talalay [21]. This method has been described in detail in many articles [22–26]. Interestingly, all CI values of JD plus PTX in the tested combination groups were <1 (Fig. 1e), which indicated that all of the tested combination groups showed a synergistic effect. The smaller the CI value was, the stronger the synergistic efficacy. It was evident that the best combination of concentrations was 20 μM JD and 5 nM PTX (Table 2), which was used in the subsequent experiments. The CI value was the ratio of the combination dosage and the sum of single-agent doses at an ISO effective level. $CI < 1$ indicated synergy, $CI > 1$ indicated antagonism, and $CI = 1$ indicated additivity.

The results above indicated that JD could enhance the efficacy of low-dose PTX by decreasing the viability of MKN45 cells. Therefore, JD plus low-dose PTX showed a synergistic effect.

Combined JD and low-dose PTX treatment synergistically inhibit colony formation

Based on the above findings, MKN45 cells were treated with 0.6 μM JD, 0.1 nM PTX or 0.6 μM JD plus 0.1 nM PTX for 7–10 days. An exciting finding was that the colonies subjected to combination treatment were smaller and fewer in number than those subjected to either agent treatment alone (Fig. 1f). The inhibition rate of colony formation was markedly increased after combined treatment (Fig. 1g), demonstrating that combined treatment with JD and low-dose PTX plays a synergistic effect on inhibiting colony formation.

JD enhances low-dose PTX-induced apoptosis of MKN45 cells in vitro

To further explore whether the suppression of cell proliferation was caused by the induction of apoptosis, annexin-V/propidium iodide (PI) double staining was performed to evaluate cell apoptosis. MKN45 cells were treated for 24 h with either no drugs as a control or with 20 μM JD alone, 5 nM PTX alone or 20 μM JD plus 5 nM PTX. Based on the results of flow cytometry, JD plus PTX showed a significant increase in the percentage of cell apoptosis (58.7 ± 2.12 %) compared to monotherapy with JD (22.8 ± 1.65 %) and with PTX (14.1 ± 1.24 %) (Fig. 2a, b).

Next, to determine the underlying mechanism of the cell apoptosis induced by combination therapy, the classical mitochondrial apoptotic pathway was first studied. A

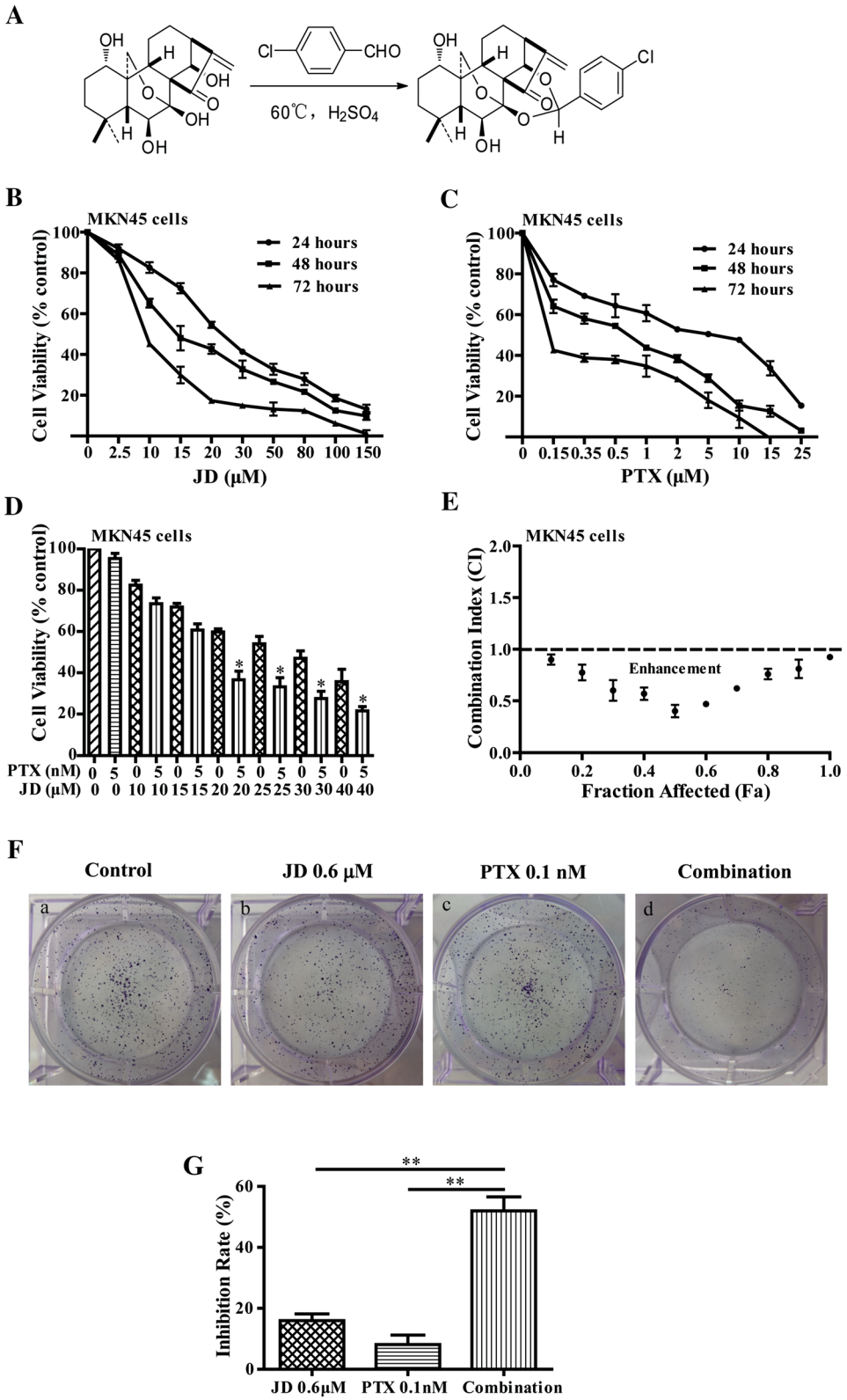

Fig. 1 **a** JD synthesis. Cell viability of MKN45 cells for JD (**b**) and PTX (**c**) treatment. **d** Cell viability of MKN45 cells for combined JD and low-dose PTX treatment. **e** The interaction relationship between JD and low-dose PTX. As described by Chou and Talay, [21] CI was plotted against the Fa, CI > 1 indicates antagonism, CI = 1 indicates additivity, and CI < 1 indicates *synergy*. Each *data point* represents at least three independently repeated experiments. **f** The effect of PTX and/or PTX on colony formation in MKN45 cells. **g** The inhibition rate of combination and single-agent treatment on MKN45 cells. *$p < 0.05$ indicates statistically significant versus either agent monotherapy. **$p < 0.01$ indicates highly statistically significant versus either agent monotherapy

Table 1 IC_{50} values for cell viability with JD and PTX treatment

Drug	IC_{50} (μM)		
	24 h	48 h	72 h
JD	27.55 ± 1.50	16.57 ± 0.24	8.49 ± 0.51
PTX	2.81 ± 0.32	0.78 ± 0.07	0.12 ± 0.02

series of pro- and anti-apoptotic proteins were examined by Western blotting after MKN45 cells were incubated with JD (20 μM), PTX (5 nM) or a combination of the two. The Bcl-2 family plays a vital role in the mitochondrial apoptotic pathway, mainly because of its impact on mitochondrial membrane permeability, membrane potential and caspase family protein members. After combination therapy, we detected higher levels of Bax and lower levels of Bcl-2 and Bcl-2/Bax than were observed with either JD or PTX monotherapy (Fig. 2c, d). Furthermore, the expression of other Bcl-2 family members, such as Bcl-xL, Mcl-1, t-Bid and Puma, was also detected. These results indicated that JD plus PTX synergistically down-regulated the expression levels of Bcl-xL and up-regulated the expression levels of t-Bid and Puma. As downstream molecules of the mitochondrial apoptotic pathway, caspase 9 and caspase 3 were markedly activated in the combined therapy compared to monotherapy (Fig. 2c, d). The results above suggest that MKN45 cell apoptosis caused by JD plus low-dose PTX could occur through the mitochondrial signalling pathway.

To further confirm our results, we added a caspase 9 inhibitor to the combination treatment with JD plus low-dose PTX. As a result, the caspase 9 inhibitor partially rescued JD plus PTX-induced apoptosis (Fig. 2e, f). Consistent with this finding, the apoptosis induced by JD plus PTX was partially reversed when Bax was knocked down by Bax-specific siRNA (Fig. 2g, h). These results indicated that the activation of the mitochondrial pathway is a mechanism that occurs in the apoptosis induced by JD and low-dose PTX. All of the data described above confirmed our finding that the mitochondrial pathway was a critical mechanism in the JD plus low-dose PTX-induced apoptosis.

In vivo, JD potentiates the anti-neoplastic effect of low-dose PTX in mice bearing MKN45 tumours

As combination treatment was superior to either JD or PTX monotherapy in vitro, we expected that it would further suppress tumour growth in vivo. To confirm these speculations, nude mice with MKN45 cell xenografts were randomised into five groups: control, JD (20 mg/kg/day), PTX (5 mg/kg/3 days), combination and PTX (10 mg/kg/3 days), which were injected in the vena caudalis. Tumour tissues were removed and photographed on the 21st day (Fig. 3a). The tumours were also weighed (Fig. 3b). Both JD and PTX showed a significant anti-tumour effect. Additionally, the combination of JD and half-dose PTX expressed a synergistic inhibitory effect similar to normal-dose PTX on the tumour volume compared with either agent treatment alone (Fig. 3c), and the body weight of the mice remained stable with no significant differences in any of the groups (Fig. 3d). The concentration of hemameba in the blood of the mice indicated that high doses of PTX (10 mg/kg/3 days) significantly reduced the number of hemameba, whereas JD (20 mg/kg/day), PTX (5 mg/kg/3 days) and the combination therapy had no obvious difference compared to the control group (Table 3). Biochemical serum analysis of alanine transaminase (ALT) and aspartate transaminase (AST) indicated no obvious effects on liver function in monotherapy mice or combination therapy mice (Tables 4, 5).

The results above suggest that combination therapy with JD and low-dose PTX could represent not only an efficient but also a safe approach to the treatment of MKN45 tumours.

In vivo, JD potentiates low-dose PTX-induced apoptosis

To assess whether the inhibitory effect on tumour growth induced by JD plus low-dose PTX was due to an increase in apoptotic cell death, haematoxylin and eosin (HE) and TUNEL staining assays were performed. HE staining exhibited increased necrosis in the group treated with JD and low-dose PTX compared with the control group (NaCl, 0.9 %), and TUNEL staining demonstrated greater apoptosis in the combination group than in either monotherapy group (Fig. 3e). These results suggested that the induction of apoptosis contributed to tumour growth inhibition.

The underlying apoptotic mechanism induced by combination therapy in vivo was further studied. We extracted total protein from the tumour tissue of the control group and the treatment groups for Western blotting. Consistent with the in vitro results, JD (20 mg/kg/day) plus PTX (5 mg/kg/3 days) activated Bax, t-Bid, Puma, cleaved-caspase 9 and cleaved-caspase 3 to a greater extent than either

Table 2 Combination index (CI) values of combined JD and PTX

PTX	JD (μM)					
(nM)	10	15	20	25	30	40
5	0.65 ± 0.05	0.57 ± 0.14	0.47 ± 0.10	0.60 ± 0.15	0.73 ± 0.12	0.82 ± 0.18

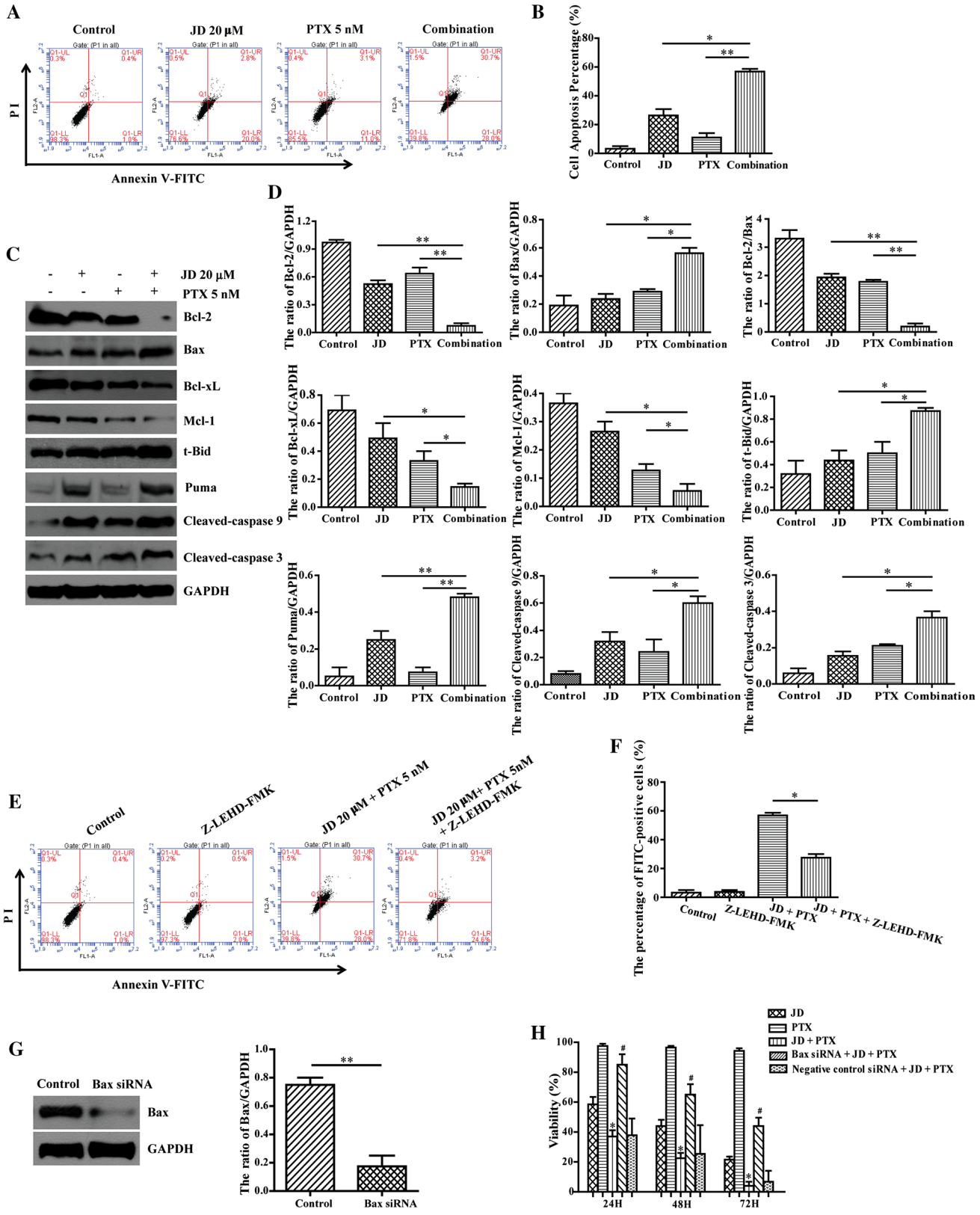

Fig. 2 JD and/or low-dose PTX induce apoptosis in vitro. **a** and **b** MKN45 cell apoptosis was analysed by the FACS technique. **c**, **d** The expression of mitochondrial apoptotic pathway-related proteins. **e**, **f** The effect of a caspase 9 inhibitor on JD plus PTX-induced cell apoptosis. **g**, **h** The efficiency of Bax knockdown. Data are the mean ± SEM. $^{*}p < 0.05$ indicates statistically significant versus either agent monotherapy. $^{**}p < 0.01$ indicates highly statistically significant versus either agent monotherapy. $^{\#}p < 0.05$ indicates highly significant versus JD + PTX

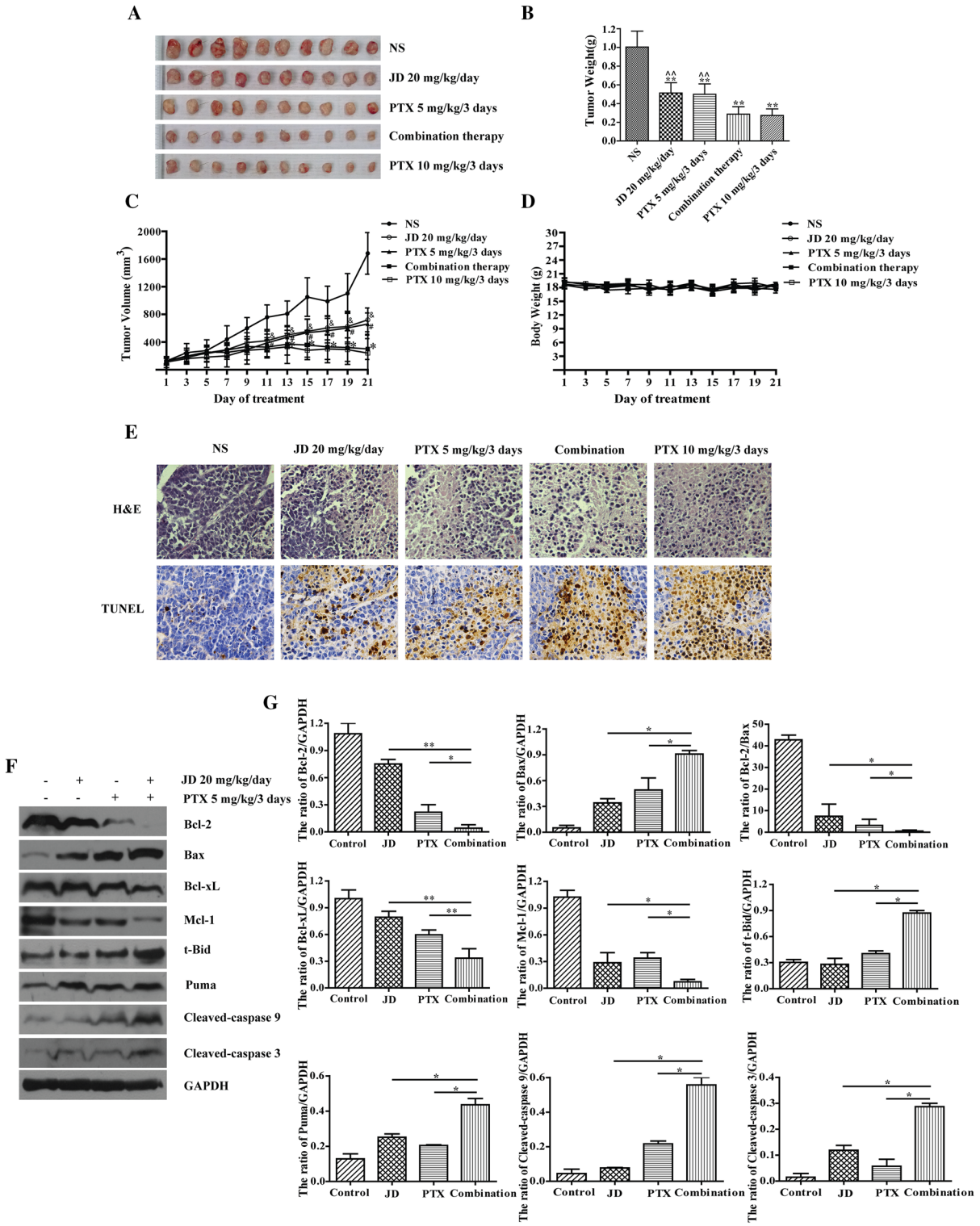

Fig. 3 Anti-tumour effects of JD plus low-dose PTX in MKN45 tumour-bearing nude mice in vivo. **a** A photograph of MKN45 xenograft tumour tissues after the mice were killed. **b** The average tumour weight was calculated when the mice were killed. The tumour weight was expressed as the mean ± SEM. $^{**}p < 0.01$ indicates statistically significant versus negative control. $^{\wedge\wedge}p < 0.01$ indicates highly statistically significant versus combination therapy. **c** The tumour volumes were graphed against the days of the experiment. $^{\&}p < 0.05$ indicates statistically significant versus negative control. $^{\#}p < 0.05$ indicates statistically significant versus negative control. $^{*}p < 0.05$ indicates statistically significant versus negative control. **d** The body weight of the mice was graphed against the days of the experiment. **e** H&E and TUNEL staining. **f**, **g** Expression of mitochondrial apoptotic pathway-related proteins after treatment with JD and/or low-dose PTX in tumour tissue. Data are the mean ± SEM. $^{*}p < 0.05$ indicates statistically significant versus either agent monotherapy. $^{**}p < 0.01$ indicates highly statistically significant versus either agent monotherapy

agent treatment alone, and JD plus PTX down-regulated Bcl-2, Bcl-xL and Mcl-1 to a lesser degree than either agent treatment alone (Fig. 3f, g). These results implied that the mitochondrial pathway is a mechanism of the JD plus PTX-induced apoptosis in vivo.

Based on the findings described above, the results indicated that the mitochondrial pathway contributed to the synergistic apoptotic effect on MKN45 gastric cancer cells that was induced by the combination of JD and PTX both in vitro and in vivo. The potential apoptotic pathways are shown in a schematic (Fig. 4).

Discussion

Multiple studies have reported the anti-tumour effects of PTX in treating gastric cancer [27, 28]. Nevertheless, despite initial responses, serious side effects and drug resistance are known to occur with increasing dosage, thus limiting the dosage and therapeutic effects of PTX [29]. Combination therapy is an important clinical administration regimen because it can effectively reduce the dose, decrease toxicity, delay the development of resistance and improve the efficacy of drug treatment [30–33].

Because JD decreased the viability of MKN45 cells in a dose- and time-dependent manner, JD seems to be a promising agent for the treatment of gastric cancer. This conclusion is based on MTT measurements, which directly correlate with the number of surviving cells. Therefore, we attempted to investigate a combination of therapeutic strategies that led to the enhancement of anti-neoplastic effects in MKN45 gastric cancer by combining JD and PTX.

We first studied the effect of either JD or PTX monotherapy on MKN45 cell viability because combined therapy is performed based on the results of monotherapy. Consistent with other reports, [34] the results demonstrated that PTX monotherapy decreased the viability of MKN45 cells in a dose- and time-dependent manner, as did JD. We also showed that the combination of JD and PTX exhibited synergy at various concentrations, of which 20 μM JD and 5 nM PTX combination was the best. Similar to the improvements in cytotoxic efficacy of PTX in various cancers that were reported in previous literature [35–38] data from the MKN45 cells treated with combined therapy indicated that JD markedly enhanced the cytotoxic effects of PTX. Recent data have suggested that the activation of the caspase cascade is clearly an important mechanism in inducing apoptosis in response to chemotherapy [39]. At present, two major apoptotic pathways that lead to caspase activation have been characterised: one is the extrinsic death receptor pathway, and the other is the intrinsic mitochondrial pathway. The extrinsic pathway is triggered by death receptors. The intrinsic pathway is controlled by Bcl-2 family members and the caspase cascade [40–42]. When the mitochondrial membrane is broken, cytochrome c is released, resulting in the caspase cascade and induction of apoptosis. Based on the increasing percentage of cell apoptosis in combination therapy compared to JD and PTX monotherapy, the molecular mechanism behind the synergism between JD and PTX was next determined by evaluating the effects of combination therapy on apoptosis-related proteins. As expected, combined therapy activated pro-apoptotic proteins, such as Bax, Puma, cleaved-caspase 3 and cleaved-caspase 9, to a greater degree and decreased anti-apoptotic proteins, such as Bcl-2, Mcl-1 and Bcl-xL, to a lower degree than either JD or PTX treatment alone. This finding was consistent with the corresponding protein levels in vivo. Moreover, both Bax siRNA knockdown and a caspase 9 inhibitor reversed the synergistic apoptosis induced by the combination of JD and PTX. These findings suggest that the intrinsic mitochondrial apoptotic pathway is involved in JD plus PTX-induced apoptosis in MKN45 gastric cancer cells.

In our in vivo pilot studies, the combined therapy in mice bearing MKN45 tumours indicated that 20 mg/kg/day of JD combined with 5 mg/kg/3 days of PTX was more effective in inhibiting MKN45 xenograft growth and inducing

Table 3 Concentration of hemameba ($\times 10^3/mm^3$) in the blood of the mice shown as the mean ± SEM

	Groups				
	NS	JD20	PTX5	Combination	PTX10
Hemameba	3.04 ± 0.82	2.67 ± 0.83	2.72 ± 0.67	3.28 ± 0.90	1.53 ± 0.25**

** $p < 0.01$ indicates statistically significant versus negative control

Table 4 Concentration of ALT (U/L) in the serum of the mice shown as the mean ± SEM

	Groups				
	NS	JD20	PTX5	Combination	PTX10
ALT	68.25 ± 2.20	78.60 ± 3.20	75.50 ± 3.19	81.15 ± 2.01	64.55 ± 2.56

Table 5 Concentration of AST (U/L) in the serum of the mice shown as the mean ± SEM

	Groups				
	NS	JD20	PTX5	Combination	PTX10
AST	206.5 ± 4.68	212.5 ± 3.66	206.0 ± 3.94	222.0 ± 5.58	218.0 ± 2.91

apoptosis than monotherapy with either agent. The combination of JD and a half-dose of PTX demonstrated a synergistic inhibitory effect similar to normal-dose PTX on tumour inhibition compared with either treatment alone. Moreover, the body weight of the mice remained stable in both treatment groups and in the control group, indicating that combined therapy with JD and low-dose PTX could represent not only an efficient but also a safe approach for the treatment of MKN45 gastric cancer.

In conclusion, our results show for the first time that JD and low-dose PTX combine synergistically in the treatment of MKN45 gastric cancer, which is attributed to mitochondrial pathways. JD enhances the anti-tumour activity of low-dose PTX in MKN45 gastric cancer cells by promoting cell apoptosis through the mitochondrial pathway. This result is what we expected to achieve with lower doses of paclitaxel combined with JD, both an increased efficacy and a reduction in toxicity. Collectively, the data we gathered in vitro, together with that collected in vivo, provide a strong and compelling rationale not only for developing novel promising therapeutic strategies to enhance the effects of classical chemotherapy but also for conducting further studies to improve the clinical outcomes of gastric cancer patients.

Materials and methods

Chemicals and experimental reagents

JD was obtained from the pharmaceutical department of Zhengzhou University and was synthesised through optimising the structure of oridonin isolated from *R. rubescens* (Fig. 1a). The synthetic pathway is described below. A mixture of oridonin and chlorobenzaldehyde was heated to 60 °C with stirring throughout the process. One drop of concentrated sulphuric acid was then added to the reaction system, which was stirred for an additional hour, followed by cooling to room temperature, two extractions with saturated Na_2CO_3 and drying over anhydrous Na_2SO_4. Finally, the reaction system was distilled and recrystallised from methanol, and the target compound was obtained. The obtained JD was a white powder with a purity of >98 % and an mp of 128–130 °C. Its chemical structure was confirmed by NMR, IR and MS analysis. Purity was detected by HPLC, and 99.9 % pure JD was used in the experiments. JD was dissolved in dimethyl sulfoxide (DMSO), and the concentration of DMSO in the culture medium was less than 0.1 % (v/v). Foetal bovine serum and RPMI-1640 culture medium were obtained from HyClone Laboratories (Utah, USA). PTX for injection (5 ml:30 mg) was purchased from Hainan Chuntch Pharmaceutical Co. Ltd. (Hainan, China). The annexin-V-FITC apoptosis detection kit was purchased from KeyGen Biotech (Nanjing, China). The primary antibodies for Bax, Bcl-2, cleaved-caspase 3 and cleaved-caspase 9 were rabbit monoclonal antibodies purchased from Abcam Biotechnology (Cambridge, UK). The primary antibodies for t-Bid, Puma, Bcl-xL and Mcl-1 were rabbit polyclonal antibodies supplied by EnoGene Biotechnology (Nanjing, China), and a GAPDH rabbit polyclonal antibody was purchased from KeyGen Biotech (Nanjing, China).

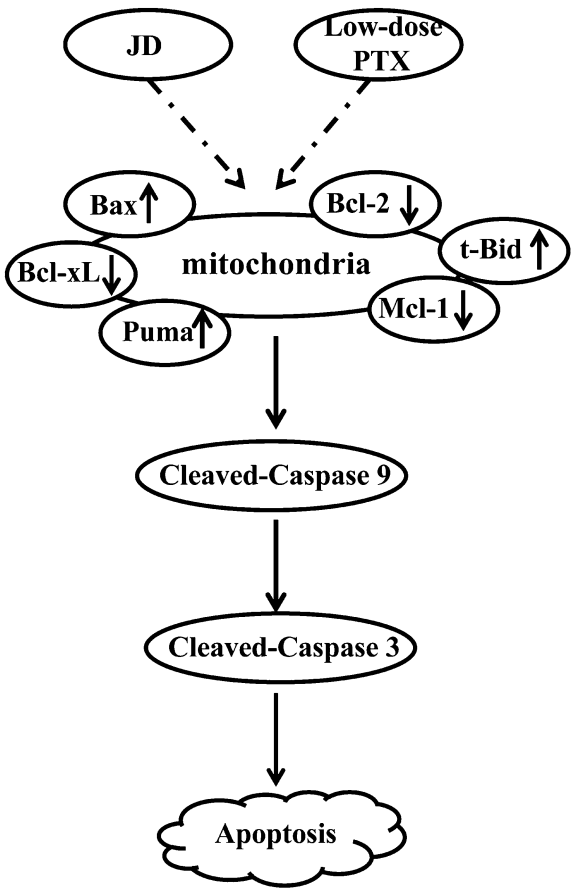

Fig. 4 Possible apoptotic pathways are summarised in the schematic

Cell lines and cell culture

The human gastric cancer cell line MKN45 was obtained from the Cell Line Bank of Shanghai Institute. Cells were cultured in RPMI-1640 containing 10 % foetal bovine serum, 100 μg/ml streptomycin and 100 U/ml penicillin G incubated at 37 °C and 5 % CO_2 in a water-saturated atmosphere.

Cell viability assay

Cell viability was estimated using the 3-(4,5-dimethylthiazol-2-yl)-2,5-diphenyltetrazolium bromide (MTT) assay. MKN45 cells were seeded in 96-well plates with an initial cell density of 7×10^3 cells/well, 5.5×10^3 cells/well or 4×10^3 cells/well. The cells were allowed to attach for 24 h at 37 °C, and then, fresh medium with different concentrations of JD ranging from 0.15 to 25 μM or paclitaxel ranging from 2.5 to 150 μM was introduced. Six deputy wells were then seeded for each concentration and incubated for 24, 48 or 72 h, corresponding to the number of seeding cells. For the combination therapy groups, the administration of JD and PTX was as previously described, except that the JD or PTX concentration was doubled and the amount added to the wells was halved. At the indicated time points, 20 μl MTT (5 mg/ml) reagent was added to each well and incubated at 37 °C for 4 h. Then, the medium was discarded, and 150 μl of DMSO was added. After shaking for 10 min, the absorbance was measured at a wavelength of 570 nm to reflect the number of living cells. Finally, the data were analysed with SPSS 20. This method detects blue formazan crystals adhering to the cells, which are generated by succinate dehydrogenase converting MTT in metabolically active cells. Under the same conditions, three independent experiments were conducted in triplicate.

Colony formation assay

A colony formation assay was performed as follows: MKN45 cells were seeded in 6-well tissue culture plates at a density of 1500 cells per well and allowed to adhere overnight. Then, the culture medium was replaced with fresh culture medium containing JD, PTX or a combination of both. During colony growth, the culture medium was replaced every 3 days. After 7–10 days, cell culture was terminated when the colonies became clearly visible (containing more than 50 cells). Next, all of the cells were fixed by methanol with 1 ml per well and then stained with 0.1 % crystal violet. The number of individual colonies was counted using the software Image J (developed by the National Institutes of Health). The inhibition rate = (1−the number of colonies in the treatment group/the number of colonies in the control group) × 100 %.

Western blotting analysis

Western bloting is a technique used to detect specific proteins that are separated by electrophoresis with labelled antibodies. We can use this technique to identify a target protein in a complex mixture and also to measure the target protein's expression level. After drug treatment, at the indicated time, all cells were washed three times with cold phosphate-buffered saline (PBS) and harvested. Suspended cells were placed on ice for 30 min in a RIPA buffer, protease inhibitor, phosphatase inhibitor and PMSF, and then, the supernatant was collected at high speed (15,000 rpm) for 15 min at 4 °C. The samples were heated at 95 °C for 10 min before being loaded onto the gel. Total protein samples were separated by 8–15 % SDS-PAGE and transferred to a 0.22 μM nitrocellulose filter membrane. Thereafter, the membranes were blocked with 5 % non-fat milk in PBS at room temperature for 2 h while shaking, hybridised with primary antibody at 4 °C overnight and then incubated with a horseradish peroxidase-linked secondary antibody for an additional 2 h at room temperature. The protein side of the membrane was exposed to X-ray film, and the protein signals were captured on Kodak X-AR film using an ECL kit.

Flow cytometry analysis

Annexin-V/propidium iodide (PI) double staining is one of the most common methods of detecting apoptosis. MKN45 cells were harvested (EDTA-free trypsin), rinsed three times with ice-cold phosphate-buffered saline (PBS), centrifuged at 2000 rpm for 5 min, placed in suspension in 500 μl binding buffer, mixed with 5 μl annexin-V-FITC and 5 μl propidium iodide and incubated for 15 min at room temperature away from light. Apoptosis was then detected using flow cytometry in 1 h (488 nm excitation wavelength, 530 nm emission wavelength). The analysis standard was as follows: annexin-V-negative and PI-negative cells were identified as normal cells, annexin-V-positive and PI-negative cells were identified as early apoptotic cells, and annexin-V- positive and PI-positive cells were identified as late apoptotic cells.

siRNA transfection assay

Twenty-four hours before transfection, cells (50×10^3 cells/well) were seeded in 6-well plates. Following 24 h of incubation, cells reached close to 80 % density and were transiently transfected with Bax-specific siRNA using Lipofectamine RNAiMAX (Invitrogen; Thermo Fisher Scientific, Inc.) according to the manufacturer's instructions. After transfection, cells were treated for an additional 24 h until the time of analysis, when they were harvested and divided into two groups. One group was used to detect the

knockdown efficiency using Western blot, and the other was used to conduct cell viability experiments with MTT. The sequences for Bax siRNA (Invitrogen; Thermo Fisher Scientific, Inc.) were as follows: Bax (sense: 5′-CAUCAGAUGUGGUCUAUAATT-3′, antisense: 5′-UUAUAGACCACAUCUGAUGTT-3′) and negative control (sense: 5′-UUCUCCGAACGUGUCACGUTT-3′, antisense: 5′-ACGUGACACGUUCGGAGAATT -3′).

Animals and tumour xenograft model

Nude female mice approximately 5–6 weeks old were supplied by Hunan SJA Animal Laboratory Co. Ltd. (Hunan, China). The mice were raised in a sterile environment and received adequate water and food. Throughout the trial period, all of the experiments strictly followed institutional guidelines and were approved by the Experimental Animal Care Committee of Zhengzhou University. For the xenograft models, 5×10^7 MKN45 gastric cancer cells were subcutaneously implanted into the right scapula of the mice. When the tumours reached 100 mm^3, the mice were randomly divided into a negative control (NaCl, 0.9 %) and treatment groups. The treatment groups included the JD group (20 mg/kg/day), PTX group (5 mg/kg/3 days), combination group (combined administration of the above dosages of PTX and JD) and PTX group (10 mg/kg/3 days). All of the treatment groups received administration for a period of 21 days, during which the body weight, tumour growth and tumour volumes of the mice were monitored and recorded each day. On the 21st day, blood samples were drawn from the orbit before the mice were killed and immediately used for white blood cell count and biochemical serum analysis of alanine transaminase (ALT) and aspartate transaminase (AST). Then, the mice were euthanised, and their tumours were removed and weighed. The tumour volumes were calculated with the following formula: tumour volume = A × B × B/2, where A was the longest dimension and B was the shortest dimension. The inhibition rate = (1−treated tumour average weight/untreated tumour average weight) × 100 %. Each tumour was divided in two: one half was stored at −80 °C, and the other half was fixed in 4 % buffered paraformaldehyde for further studies.

Haematoxylin and eosin (HE) and TUNEL assays

Haematoxylin and eosin (HE) staining was used to identify normal and pathological tissue. Tumour tissues acquired from the tumour-bearing mice were fixed in 4 % buffered paraformaldehyde for 24 h. Pure paraffin was chosen to embed the tumour tissues. Paraffin-embedded tumour tissues were cut into 4-μm sections, affixed to glass slides, deparaffinised in xylene, rehydrated in ethanol, rinsed in distilled water and then fixed with 4 % formaldehyde. Thereafter, the paraffin sections were stained with haematoxylin and eosin, dehydrated in graded alcohol, cleared in xylene, cemented with neutral resin and finally analysed under a light microscope. The TUNEL reaction preferentially labels DNA strand breaks that are generated during apoptosis. This allows the discrimination of apoptosis from necrosis and from primary DNA strand breaks induced by cytostatic drugs or by irradiation. TUNEL staining was performed according to the manufacturer's protocol with an apoptosis detection kit (Roche, California, USA). First, the paraffin-embedded tissue sections were dewaxed. The tissue sections were then incubated for 15–30 min at 21–37 °C with a proteinase K working solution and then incubated with the TUNEL reaction solution according to the kit. DAB application was used to evaluate tissue peroxidase activity. After the substrate reaction occurred, the samples were analysed under a light microscope.

Statistical analysis

One-way analysis of variance (ANOVA) (comparing more than 2 means) and Student's *t* test (comparing two means) was performed to assess the statistical significance of differences between different groups. The data were expressed in the form of mean ± SEM. p values <0.05 were considered statistically significant, and p values <0.01 were highly significant.

Acknowledgments This work was supported by the National Natural Science Foundation of China (Project No.81430085, 21372206 and 81172937 for Hongmin Liu), the Natural Science Foundation of He'nan Province of China (Project No.152300410030 for Cong Wang), the Science and Technology Research Key Project in the Henan province Department of Education (Project No.14B350011 for Cong Wang).

Compliance with ethical standards

Conflict of interest No potential conflicts of interest were disclosed.

References

1. Lin X, Zhao Y, Song W, Zhang B (2015) Molecular classification and prediction in gastric cancer. Comput Struct Biotechnol J 13:448–458. doi:10.1016/j.csbj.2015.08.001
2. Xu W, Yang Z, Lu N (2016) Molecular targeted therapy for the treatment of gastric cancer. J Exp Clin Canc Res 35(1):324–341. doi:10.1186/s13046-015-0276-9
3. Rahman R (2014) Characteristics of gastric cancer in Asia. World J Gastroenterol 20:4483–4496. doi:10.3748/wjg.v20.i16.4483
4. Frese KK, Neesse A, Cook N, Bapiro TE, Lolkema MP, Jodrell DI, Tuveson DA (2012) nab-Paclitaxel potentiates

gemcitabine activity by reducing cytidine deaminase levels in a mouse model of pancreatic cancer. Cancer Discov 2:260–269. doi:10.1158/2159-8290.CD-11-0242
5. Azzarito T, Venturi G, Cesolini A, Fais S (2015) Lansoprazole induces sensitivity to suboptimal doses of paclitaxel in human melanoma. Cancer Lett 356:697–703. doi:10.1016/j.canlet.2014.10.017
6. Volk LD, Flister MJ, Chihade D, Desai N, Trieu V, Ran S (2011) Synergy of nab-paclitaxel and bevacizumab in eradicating large orthotopic breast tumors and preexisting metastases. Neoplasia 13:314–327. doi:10.1593/neo.101490
7. Bhuvaneswari R, Ng QF, Thong PS, Soo KC (2015) Nimotuzumab increases the anti-tumor effect of photodynamic therapy in an oral tumor model. Oncotarget 6:13487–13505. doi:10.18632/oncotarget.3622
8. Rebecca VW, Massaro RR, Fedorenko IV, Sondak VK, Anderson ARA, Kim E, Amaravadi RK, Maria-Engler SS, Messina JL, Gibney GT, Kudchadkar RR, Smalley KSM (2014) Inhibition of autophagy enhances the effects of the AKT inhibitor MK-2206 when combined with paclitaxel and carboplatin in BRAF wild-type melanoma. Pigment Cell Melanoma Res 27:465–478. doi:10.1111/pcmr.12227
9. Ahmed AA, Wang X, Lu Z, Goldsmith J, Le XF, Grandjean G, Bartholomeusz G, Broom B, Bast RC (2011) Modulating microtubule stability enhances the cytotoxic response of cancer cells to paclitaxel. Cancer Res 71:5806–5817. doi:10.1158/0008-5472.CAN-11-0025
10. Ingemarsdotter CK, Baird SK, Connell CM, Oberg D, Hallden G, McNeish IA (2010) Low-dose paclitaxel synergizes with oncolytic adenoviruses via mitotic slippage and apoptosis in ovarian cancer. Oncogene 29:6051–6063. doi:10.1038/onc.2010.335
11. Isham CR, Bossou AR, Negron V, Fisher KE, Kumar R, Marlow L, Lingle WL, Smallridge RC, Sherman EJ, Suman VJ, Copland JA, Bible KC (2013) Pazopanib enhances paclitaxel-induced mitotic catastrophe in anaplastic thyroid cancer. Sci Transl Med 5:163–166. doi:10.1126/scitranslmed.3004358
12. Jin H, Park MH, Kim SM (2015) 3,3′-Diindolylmethane potentiates paclitaxel-induced antitumor effects on gastric cancer cells through the Akt/FOXM1 signaling cascade. Oncol Rep 33:2031–2036. doi:10.3892/or.2015.3758
13. Bocci G, DiPaolo A, Danesi R (2013) The pharmacological bases of the antiangiogenic activity of paclitaxel. Angiogenesis 16:481–492. doi:10.1007/s10456-013-9334-0
14. Jeong J, Kim K, Moon J, Song J, Choi S, Kim K, Kim T, An H (2013) Targeted inhibition of phosphatidyl inositol-3-kinase p110β, but not p110α, enhances apoptosis and sensitivity to paclitaxel in chemoresistant ovarian cancers. Apoptosis 18:509–520. doi:10.1007/s10495-013-0807-9
15. Mitsuuchi Y, Johnson SW, Selvakumaran M, Williams SJ, Hamilton TC, Testa JR (2000) The phosphatidylinositol 3-kinase/AKT signal transduction pathway plays a critical role in the expression of p21WAF1/CIP1/SDI1 induced by cisplatin and paclitaxel. Cancer Res 60:5390–5394. doi:10.1186/1744-8069-10-61
16. Hu J, Zhang NA, Wang R, Huang F, Li G (2015) Paclitaxel induces apoptosis and reduces proliferation by targeting epidermal growth factor receptor signaling pathway in oral cavity squamous cell carcinoma. Oncol Lett 10:2378–2384. doi:10.3892/ol.2015.3499
17. Zhou HB, Zhu JR (2003) Paclitaxel induces apoptosis in human gastric carcinoma cells. World J Gastroenterol 9:442–445
18. Ma Y, Su N, Shi X, Zhao W, Ke Y, Zi X, Zhao N, Qin Y, Zhao H, Liu H (2015) Jaridonin-induced G2/M phase arrest in human esophageal cancer cells is caused by reactive oxygen species-dependent Cdc2-tyr15 phosphorylation via ATM–Chk1/2–Cdc25C pathway. Toxicol Appl Pharmacol 282:227–236. doi:10.1016/j.taap.2014.11.003
19. Wang C, Jiang L, Wang S, Shi H, Wang J, Wang R, Li Y, Dou Y, Liu Y, Hou G, Ke Y, Liu H (2015) The antitumor activity of the novel compound jesridonin on human esophageal carcinoma cells. PLoS One 10:1302–1315. doi:10.1371/journal.pone.0130284
20. Kang N, Cao SJ, Zhou Y, He H, Tashiro S, Onodera S, Qiu F, Ikejima T (2015) Inhibition of caspase-9 by oridonin, a diterpenoid isolated from Rabdosia rubescens, augments apoptosis in human laryngeal cancer cells. Int J Oncol 47:2045–2056. doi:10.3892/ijo.2015.3186
21. Chou TC, Talalay P (1984) Quantitative analysis of dose-different relationships: the combined effects of multiple drugs or enzyme and inhbitors. Adv Enzyme Regul 22:27–55
22. Solit DB, Basso AD, Olshen AB, Scher HI, Rosen N (2003) Inhibition of heat shock protein 90 function down-regulates Akt kinase and sensitizes tumors to Taxol. Cancer Res 63:2139–2144
23. Ricotti L, Tesei A, De Paola F, Ulivi P, Frassineti GL, Milandri C, Amadori D, Zoli W (2003) In vitro schedule-dependent interaction between docetaxel and gemcitabine in human gastric cancer cell lines. Clin Cancer Res 9:900–905
24. Lee JG, Wu R (2015) Erlotinib-Cisplatin combination inhibits growth and angiogenesis through c-MYC and HIF-1α in EGFR-mutated lung cancer in vitro and in vivo. Neoplasia 17:190–200. doi:10.1016/j.neo.2014.12.008
25. Nagaraju GP, Alese OB, Landry J, Diaz R, El-Rayes BF (2014) HSP90 inhibition downregulates thymidylate synthase and sensitizes colorectal cancer cell lines to the effect of 5FU-based chemotherapy. Oncotarget 5:9980–9991. doi:10.18632/oncotarget.2484
26. Montraveta A, Xargay-Torrent S, Lopez-Guerra M, Rosich L, Perez-Galan P, Salaverria I, Bea S, Kalko SG, de Frias M, Campas C, Roue G, Colomer D (2014) Synergistic anti-tumor activity of acadesine (AICAR) in combination with the anti-CD20 monoclonal antibody rituximab in in vivo and in vitro models of mantle cell lymphoma. Oncotarget 5:726–739. doi:10.18632/oncotarget.1455
27. Almhanna K, Cubitt CL, Zhang S, Kazim S, Husain K, Sullivan D, Sebti S, Malafa M (2014) MK-2206, an Akt inhibitor, enhances carboplatinum/paclitaxel efficacy in gastric cancer cell lines. Cancer Biol Ther 14:932–936
28. Satoh T, Xu RH, Chung HC, Sun GP, Doi T, Xu JM, Tsuji A, Omuro Y, Li J, Wang JW, Miwa H, Qin SK, Chung IJ, Yeh KH, Feng JF, Mukaiyama A et al (2014) Lapatinib plus paclitaxel versus paclitaxel alone in the second-line treatment of HER2-amplified advanced gastric cancer in Asian populations: TyTAN—a randomized, phase III study. J Clin Oncol 32:2039–2049. doi:10.1200/JCO.2013.53.6136
29. Ikeda H, Taira N, Nogami T, Shien K, Okada M, Shien T, Doihara H, Miyoshi S (2011) Combination treatment with fulvestrant and various cytotoxic agents (doxorubicin, paclitaxel, docetaxel, vinorelbine, and 5-fluorouracil) has a synergistic effect in estrogen receptor-positive breast cancer. Cancer Sci 102:2038–2042. doi:10.1111/j.1349-7006.2011.02050.x
30. Li G, Zhao J, Peng X, Liang J, Deng X, Chen Y (2012) Radiation/paclitaxel treatment of p53-abnormal non-small cell lung cancer xenograft tumor and associated mechanism. Cancer Biother Radiopharm 27:227–233. doi:10.1089/cbr.2011.1154
31. Winterhoff B, Freyer L, Hammond E, Giri S, Mondal S, Roy D, Teoman A, Mullany SA, Hoffmann R, von Bismarck A, Chien J, Block MS, Millward M, Bampton D, Dredge K, Shridhar V (2015) PG545 enhances anti-cancer activity of chemotherapy in ovarian models and increases surrogate biomarkers such as VEGF in preclinical and clinical plasma samples. Eur J Cancer 51:879–892. doi:10.1016/j.ejca.2015.02.007
32. Sain N (2006) Potentiation of paclitaxel activity by the HSP90 inhibitor 17-allylamino-17-demethoxygeldanamycin in human

ovarian carcinoma cell lines with high levels of activated AKT. Mol Cancer Ther. doi:10.1158/1535-7163.MCT-05-0445
33. Ying L, Zhu Z, Xu Z, He T, Li E, Guo Z, Liu F, Jiang C, Wang Q (2015) Cancer associated fibroblast-derived hepatocyte growth factor inhibits the paclitaxel-induced apoptosis of lung cancer A549 cells by up-regulating the PI3 K/Akt and GRP78 signaling on a microfluidic platform. PLoS One 10:e129593. doi:10.1371/journal.pone.0129593
34. Erba PA, Manfredi C, Lazzeri E, Minichilli F, Pauwels EK, Sbrana A, Strauss HW, Mariani G (2010) Time course of paclitaxel-induced apoptosis in an experimental model of virus-induced breast cancer. J Nucl Med 51:775–781. doi:10.2967/jnumed.109.071621
35. Xu C, Li X, Li T, Wang X, Yang Y, Xiao L, Shen H (2011) Combination effects of paclitaxel with signaling inhibitors in endometrial cancer cells. Asian Pac J Cancer Prev 12(11):2951–2957
36. Shi C, Chen Q, Shen S, Wu R, Yang B, Liu Q, Xu Q (2015) Paclitaxel combined with oxaliplatin as first-line chemotherapy for locally advanced or metastatic gastric cancer. Expert Rev Anticancer Ther 15:595–601. doi:10.1586/14737140.2015.1026807
37. Jin C, Li H, He Y, He M, Bai L, Cao Y, Song W, Dou K (2010) Combination chemotherapy of doxorubicin and paclitaxel for hepatocellular carcinoma in vitro and in vivo. J Cancer Res Clin 136:267–274. doi:10.1007/s00432-009-0658-5
38. Zhang X, Zhang Y (2015) Enhanced antiproliferative and apoptosis effect of paclitaxel-loaded polymeric micelles against non-small cell lung cancers. Tumor Biol 36:4949–4959. doi:10.1007/s13277-015-3142-7
39. Ehteda A, Galettis P, Pillai K, Morris DL (2013) Combination of albendazole and 2-methoxyestradiol significantly improves the survival of HCT-116 tumor-bearing nude mice. BMC Cancer 13:86–97. doi:10.1186/1471-2407-13-86
40. Zhang X, Gu Y, Chen T, Yang D, Wang X, Jiang B, Shao K, Zhao W, Wang C, Wang J, Zhang Q, Liu H (2015) Synthesis, in vitro and in vivo anticancer activities of novel 4-substituted 1,2-bis 4-chlorophenyl)-pyrazolidine-3,5-dione derivatives. Med Chem Commun 6:1781–1786
41. Wang X, Beitler JJ, Wang H, Lee MJ, Huang W, Koenig L, Nannapaneni S, Amin AR, Bonner M, Shin HJ, Chen ZG, Arbiser JL, Shin DM (2014) Honokiol enhances paclitaxel efficacy in multi-drug resistant human cancer model through the induction of apoptosis. PLoS One 9:8636–8649. doi:10.1371/journal.pone.0086369
42. Moldoveanu T, Follis AV, Kriwacki RW, Green DR (2014) Many players in BCL-2 family affairs. Trends Biochem Sci 39:101–111. doi:10.1016/j.tibs.2013.12.006